

Research Article

Assessment of Carbon Stock in Pichavaram Mangrove Forest Using Remote Sensing And GIS

Mr. R. Ramasubu¹, Dr. S. Palanivelraja²

¹Research Scholar in the Department of Civil Engineering, Annamalai University

²Professor of Civil Engineering, Annamalai University

ABSTRACT

Mangrove forest is an essential ecosystem in coastal locations that provides vital ecological and economic functions. Mangrove forests provide a carbon sink function by sequestering CO₂ from the atmosphere through photosynthesis and carbon storage on the sediment. Carbon stored in mangrove silt will remain for millennia before returning to the atmosphere, acting as a long-term carbon sink. As a result, it is critical to comprehend the spatial and temporal distribution of carbon stored inside mangrove ecosystems. This research describes an effort to map carbon stocks in mangrove forests using remote sensing technology to overcome the limitations of field surveys. The use of medium spatial resolution Landsat 8 OLI is emphasised for mapping mangrove carbon stock. Landsat 8 OLI imageries are inexpensive, widely available, and cover a large region, making them an economic tool to map mangrove carbon reserves. Using Remote Sensing data, image processing techniques such as the Normalised Difference Vegetation Index (NDVI) are used to determine the optimum strategy for explaining variance in mangrove carbon stocks. Furthermore, This study attempted to quantify the mangrove carbon sequestration rate using multitemporal analysis. Finally, the maps of carbon stocks in the mangrove forest at Pichavaram are developed for 2015, 2018 and 2020.

Keywords: NDVI, Mangrove Forest, Carbon Storage, Remote Sensing

1.Introduction:

Carbon dioxide is one of the significant greenhouse gases found in the earth's atmosphere. In recent decades human activities have reared the concentration of carbon dioxide in the earth's atmosphere, intensifying the natural greenhouse effect. The Greenhouse-gas emission must be lowered to address the challenges of global climate change (Lehmann, 2007). Rising atmospheric CO₂ concentrations are also expected to increase CO₂ concentrations at the ocean surface due to continuous gas exchange between the air and seawater (Kurihara and Shirayama, 2004). High carbon dioxide concentrations on the ocean surface make it difficult for aquatic species to respire. Hence, the sinking of the atmospheric carbon in the land and the ocean surface is crucial in climate change.

Tropical forests are regarded as substantial terrestrial carbon stores, mainly mangroves found in the subtropics and tropics, which are extraordinarily productive and distinct from other ecosystems in the carbon sink (Ahmed and Kamruzzaman, 2021). Despite their limited distribution, mangroves can play a significant role in carbon sequestration by accumulating a large amount of organic matter in their substrata, in addition to their high underground root output (Komiyama *et al.*, 2000). In maritime India, mangroves are distributed in the estuarine environments. Sundarbans is the largest mangrove ecosystem in the country. In South India, Pichavaram has one of the largest mangrove ecosystems (Ramanathan *et al.*, 1999; Kathiresan, 2000).

In this decade, quantifying the carbon stock stored by the mangroves is much required as of the rapid climate changes. Moreover, the spatial pattern of the mangrove ecosystems is dynamic due to

anthropogenic and natural influences; quantifying carbon stored by the mangroves should be complemented with change detection. Traditionally, the data was gathered through field sampling and visual interpretation of aerial photographs. Those procedures are costly, labour-intensive, and time-consuming. Furthermore, they only monitor a subset of the area of interest. Monitoring mangrove regions with digital remote sensing provides a more rapid, repeatable, objective, and efficient method at the landscape level.

Additionally, remote-sensing methods can enable the mapping of more extensive areas by utilising the growing quantity of temporal databases of satellite imagery. Spectral indices are a standard method for monitoring biomass (Curran, 1981). Spectral indices can also be used to identify changes in carbon storage by mangroves, as carbon accounts for half of the dry-weight biomass of the species (Myeong, Nowak and Duggin, 2006). The Normalised Difference Vegetation Index (NDVI), which uses red and near-infrared reflectance data, is the most often used spectral index. This study employed NDVI based on Landsat 8 OLI imagery's red and near-infrared bands.

- The primary objectives of this study were to establish quick and low-cost methods for quantifying the above-ground carbon storage and the atmospheric CO₂ of the Pichavaram mangrove forest using Landsat 8 OLI images as an alternative to more elaborate, limiting, and expensive ground-based or photogrammetric methods and the track the evolution of carbon storage by mangroves in the Pichavaram forest throughout the years 2015, 2018 and 2020.

2. Study Area:

The Pichavaram mangrove forest is located between the Vellar and Coleroon estuaries (Figure 1). The forest is found on 51 islets varying in size from 10 m² to 2 km², which are linked together by complicated canals that connect the Vellar and Coleroon estuaries (Kathiresan, 2000). Near the Coleroon estuary, the southern section is characterised by mangrove vegetation, whereas the northern section, near the Vellar estuary, is dominated by mudflats. The mangrove encompasses an area of around 11 km², of which 50% is covered by forest, 40% by waterways, and the remainder by salt pans and mudflats (Subramanian, Jeyaseelan and Krishnamurthy, 1984).

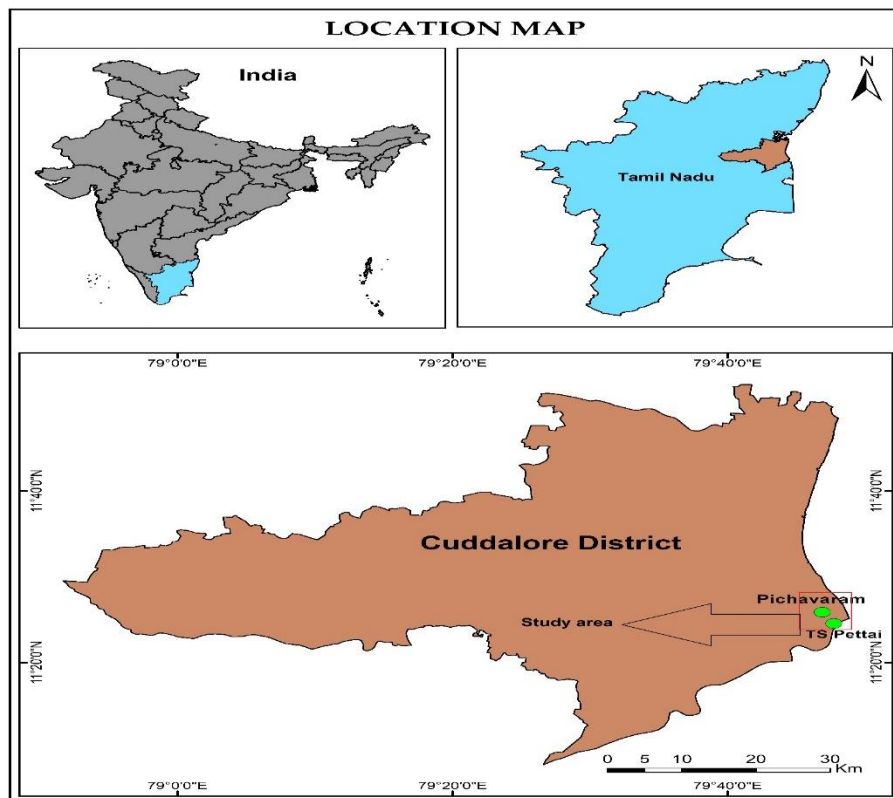


Figure 1 Location map of the study area

Pichavaram climate is sub-humid, with hot summers (> 30 Celsius) and air temperatures ranging from 20 to 38 degrees Celsius(Gnanamoorthy *et al.*, 2019). In contrast to the rest of the country, the study area receives the most rainfall during the North-East monsoon (October-December). Pichavaram seasonality is as follows: post-monsoon (January–March), summer (April–June), premonsoon (July–September), and northeast monsoon (October–December).

3. Methodology:

In this study, Landsat 8 OLI imageries were used, acquired during the summer season for the years 2015,2018 and 2020. Landsat 8 has the spectral resolution of coastal aerosol, the visible region, the near-infrared, the short infrared, panchromatic, and TIRS. The spatial resolution of bands 1 to 6 and 9 is 30m, band 7 is 60m, band 8 is 15m, and bands 10 and 11 are 100m (Table1).

Table 1 Details of the Landsat 8 OLI Imagery

BANDS	SPECTRAL RESOLUTION	SPATIAL RESOLUTION
1	Coastal aerosol	30m
2	Blue	30m
3	Green	30m
4	Red	30m
5	Near-Infrared (NIR)	30m
6	Short-wave Infrared (SWIR) 1	30m
7	Short-wave Infrared (SWIR) 2	60m
8	Panchromatic	15m
9	Cirrus	30m
10	TIRS 1	100m
11	TIRS 2	100m

ENVI 5.1 and ArcGIS 10.3 were used to process the Landsat images.Landsat image data were projected to the Universal Transverse Mercator (UTM) coordinate system, Datum WGS 1984, Zone 44North. After the projection, the 30m resolution images were converted into 15m by fusing the PAN band (8th band) with the MS(Multi-Spectral) bands. The fused image can deliver more precise and dependable data for artificial decision-making, which is advantageous for applications such as ground object classification, target recognition, and artificial visual interpretation (Li and Cheng, 2019). This fusing technique is also referred to as pansharpening (Aiazzi *et al.*, 2009). Pansharpening was carried out as Landsat series images have a limited spatial resolution (30 m) of MS image (Pardo-Pascual *et al.*, 2012).

Landsat image band combinations were utilised to detect mangroves in the study area. False Colour Composite was the name given to the band combination (FCC). The FCC used on the Landsat image was a band 7,6,4 composite; this band combination can make mangroves stand out from other things. The mangrove region was discovered and demarcated using visual interpretation and digitalisation on a screen. Following the identification of mangrove areas, the next stage was to use the NDVI transformation to categorise mangrove density into three classes.

The NDVI method was used to assess the density of mangrove forest cover. Mangrove determination was carried out through visual interpretation and delineation of objects indicating the presence of mangrove. Mangrove may be identified by using the colour combination (Red: Green:Blue), which consists of band IR (Infrared) offered at the red layer (Red), band NIR (Near Infrared) presented at the

green layer, and band Red presented at the blue layer. Mangroves appear bright red on FCC satellite pictures if they are in a continuous patch. The NDVI data layer is described as follows:

$$NDVI = (NIR - R) / (NIR + R)$$

NIR denotes spectral reflectance in the near-infrared range, and R denotes reflectance in the red band. By definition, the NDVI actual values would be between -1 and +1, increasing positive values indicating increasing green vegetation and decreasing negative values indicating non-vegetated surface features such as water, barren terrain, ice, snow, or clouds (Qi *et al.*, 1994). NDVI, Ratio of NIR and Red wavelengths, and other satellite-derived indices can also be utilised to effectively monitor the vegetation status and condition of the mangrove ecosystem (Patil *et al.*, 2015). The difference between maximum absorption of radiation in red due to chlorophyll and maximum reflection of radiation in NIR owing to leaf cellular structure is used to calculate NDVI. The combination of red and infrared (IR) bands and vegetation indices aids in identifying mangroves, swamps, and other plants in wetland zones.

3.1 Calculating the carbon storage using NDVI:

Allometric equations for Above-Ground Biomass (AGB) and Below-Ground Biomass (BGB) developed by (Komiyama, Pongpan and Kato, 2005) is used in this study.

$$AGB = 0.251 * \rho * DBH^{2.46}$$

$$BGB = 0.199 * \rho^{0.90} * DBH^{2.22}$$

where ρ is species-specific wood density.

From the field observations, BGB is also calculated, and the ratio of BGB to AGB is used to calculate BGB for the entire plot since BGB is equally important in the case of mangroves. Total biomass is taken as the sum of AGB and BGB.

The NDVI values derived from the satellite data and the AGB can be calculated using the following equation using the NDVI: (Myeong, Nowak and Duggin, 2006).

$$AGB = a * e^{(NDVI * b)}$$

a, b and e are constants determined from the nonlinear regression equation. Carbon content can be obtained by multiplying the total biomass by a conversion factor of 0.475 (47.5% of the biomass, IPCC).

4. Result and Discussion:

Mangrove density has been identified using NDVI for the years 2015, 2018 and 2020. Moreover, the data were tabulated and mapped.

4.1 NDVI and the Mangrove Density:

The density of the mangrove forest was classified into three distinct categories: High Density, Medium Density and Low Density based on their NDVI values. Mangrove class name and their NDVI range are shown in Table 2.

Table 2 Mangrove class name and their NDVI range

Class Name	NDVI range
High Density	-0.45 to -0.29
Medium Density	-0.29 to -0.25

Low Density	-0.25 <
-------------	---------

4.1.1 NDVI for the year 2015:

During the year 2015, high dense mangroves occupied 2.12 km² in the study area; During this period, the medium dense mangrove canopies had a larger extent than the high-density varieties with an area of 2.887 km² (Table 3). At the same time, low, dense canopies have less than a square kilometre extends. Figure 2 shows the NDVI map of the year 2015. The total area of the mangrove cover was estimated as 5.891km² in 2015.

Table 3 Mangrove Density for the year 2015

Mangrove Density 2015		
Mangrove Density	Area	Pixel Count
High Density	2.12	2125
Medium Density	2.887	2887
Low Density	0.884	884
	5.891	5896

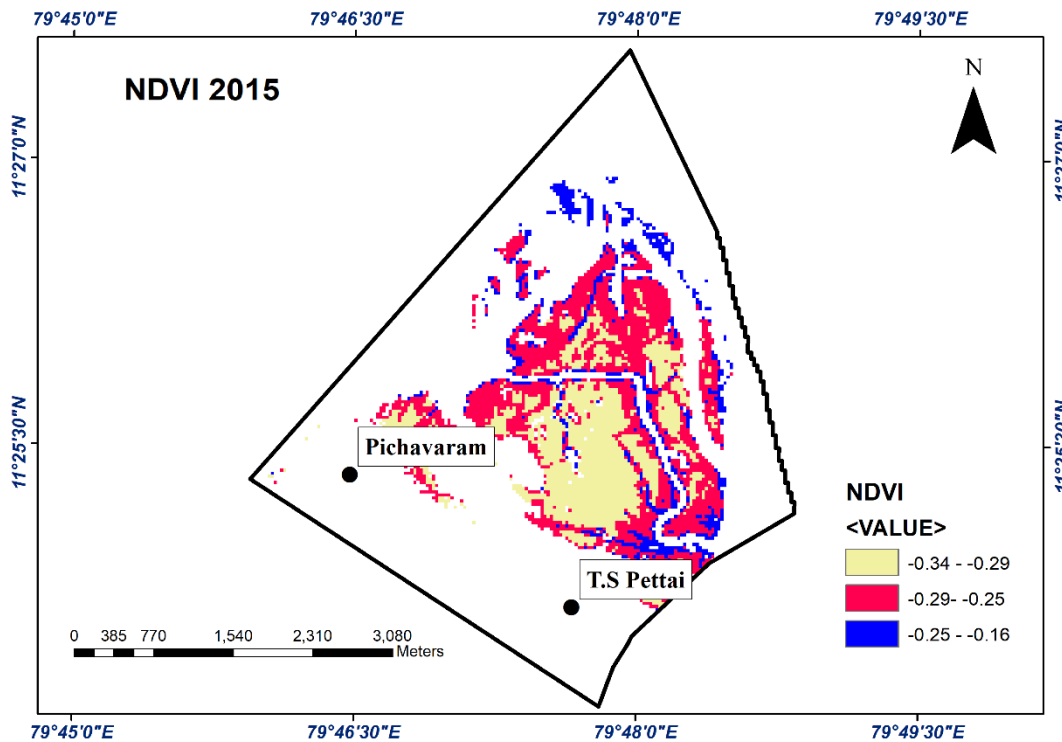


Figure 2 NDVI map for the year 2015

4.1.2 NDVI for the year 2018:

During the year 2018, high dense mangroves occupied 6 km² in the study area, and other classes had a much lower extent when compared to the high dense mangroves during the year 2018 (Table 4). Medium and low dense canopies are less than a square kilometre extended during the period. Figure 3 shows the NDVI map for the year 2018. The total area of the mangrove cover was estimated as 6.21 km² in 2018.

Table 4 Mangrove Density for the year 2018

Mangrove Density 2018		
Mangrove Density	Area	Pixel Count
High Density	6	5912
Medium Density	0.11	101
Low Density	0.09	9
	6.2	6022

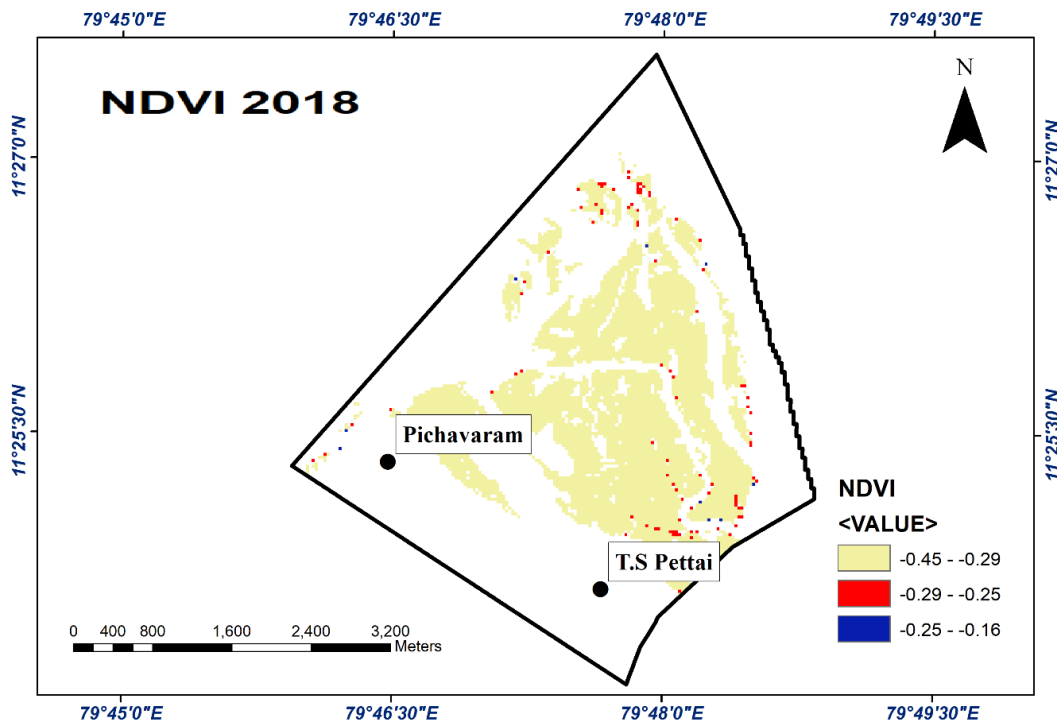


Figure 3 NDVI map for the year 2018

4.1.3 NDVI for the year 2020:

During the year 2020, high dense mangroves occupy 5.9 km² in the study area, and other classes are much lower extent when compared to the high dense mangroves during the year 2020 (Table 5). Medium and low dense canopies are less than a square kilometre extended during the period. Figure 4 shows the NDVI map for the year 2020. The total area of the mangrove cover was estimated as 6.21 km² in 2020, are like 2018.

Table 5 Mangrove Density for the year 2020

Mangrove Density 2020		
Mangrove Density	Area	Pixel Count
High Density	5.9	5889
Medium Density	0.11	113
Low Density	0.2	20
	6.21	6022

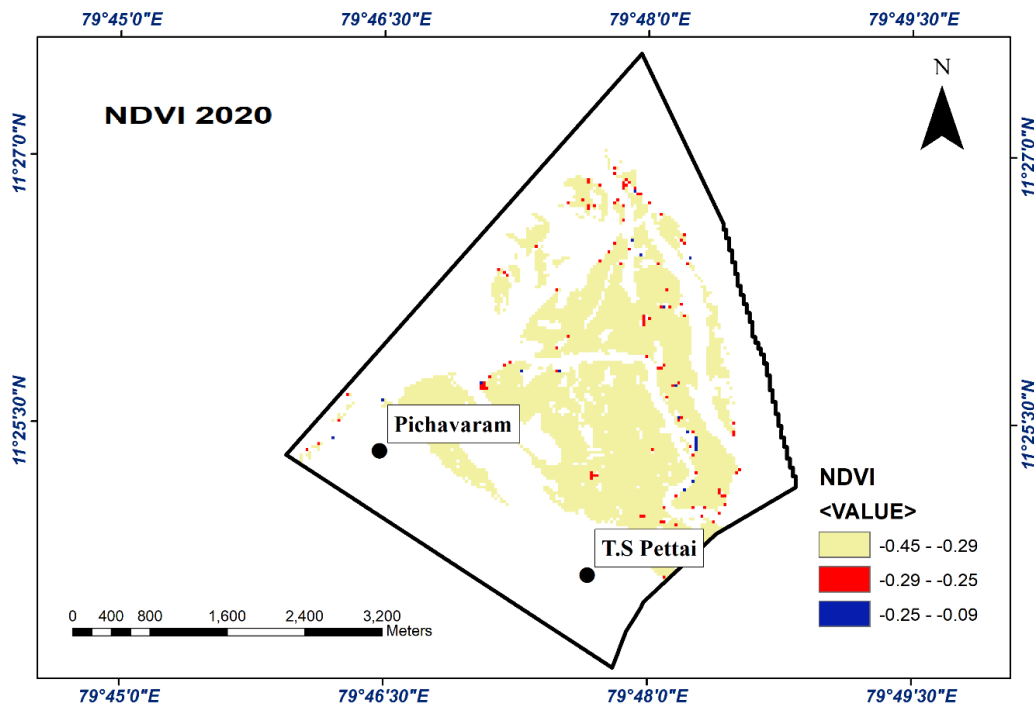


Figure 4 NDVI map for the year 2020

The ratio of AGB to BGB is calculated separately for each species, and average Value is taken. The average value of the ratio of BGB to ABG of different species in the plots is 0.38. This agrees well with the root: shoot ratios reviewed by (Yuen *et al.*, 2013).

AGB values ranging from 636.832 gm to 32048.5 gm per pixel

BGB ranging from 241.996 gm to 12178.4 gm

Total biomass ranging from 878.828 gm to 44226.9 gm

Carbon content per pixel ranges from 417.443 gm to 21007.8 gm

Carbon storage was identified for each class, and for each class's gm/pixel values were obtained.

Low Density Mangroves = 417.443 gm /pixel

Medium Density Mangroves = 10500 gm/ pixel

High Density Mangroves = 21007.8 gm /pixel**4.2.1 Carbon storage for the year 2015**

Carbon storage for the year 2015 is given in Table 6. The mangroves stored 83.02 metric tons of carbon in the study area. A large fraction of the mangroves in India was destroyed due to aquaculture, and agriculture expansion (Sahu *et al.*, 2015), especially in these places' aquaculture sites are more common than any other part of the south India. These aquaculture sites almost deforested the mangrove ecosystem. Hence these 2015, the carbon content stored by the mangroves are identified as significantly low.

Table 6 Carbon storage for the year 2015

Carbon content 2015	
Low-density mangroves	0.406 ton
Medium-density mangroves	33.414 ton
High-density mangroves	49.2 ton
Total	83.02 metric ton

4.2.2 Carbon storage for the year 2018 and 2020

Carbon storage for the years 2018 and 2020 are given in Tables 7 and 8. These two years, the carbon storage by the mangroves was almost identical because of the proper protection and measurements taken by the government organisations and the increase of local awareness. In 2018 almost 138 metric ton of carbon was stored, and in 2020, almost 138 metric ton of carbon was stored by these canopies in the study area.

Table 7 Carbon storage for the year 2018

Carbon content 2018	
Low-density mangroves	0.004 ton
Medium-density mangroves	1.16 ton
High-density mangroves	136.8 ton
Total	137.964 metric ton

Table 8 Carbon storage for the year 2020

Carbon content 2020	
Low-density mangroves	0.009 ton
Medium-density mangroves	1.30 ton
High-density mangroves	136.37 ton
Total	137.679 metric ton

5. Conclusion:

Mangroves play a more role in high carbon stock than any other forest. Landsat 8 OLI FCC are used to map mangrove carbon stock with maximum accuracy of 80 % for AGB and 75 % for BGB. This error was achieved using a vegetation index NDVI. NDVI showed consistent results across the various

level of radiometric correction compared to other vegetation indexes. Multitemporal remote sensing approach to estimate carbon sequestration rate showed a promising result. However, this study also reports the accuracy of the estimation due to the lack of field data about mangroves' carbon sequestration rate.

Nevertheless, judging from the accuracy of the carbon stock estimation of the Landsat 8 OLI image, this study assumed that the error of mangrove carbon sequestration estimation should be around that value. Finally, the map derived from remote sensing data may improve mangrove carbon stock's spatial and temporal distribution. Future work would evaluate the accuracy of carbon sequestration estimation from multitemporal analysis and involve the sediment carbon stock in mangrove areas to obtain mangrove's ecosystem carbon stock. The results show the improvement of the carbon stock from 2015 because of the proper care by the government organisations towards this canopy.

References:

1. Ahmed, S. and Kamruzzaman, M. (2021) 'Species-specific biomass and carbon flux in Sundarbans mangrove forest, Bangladesh: Response to stand and weather variables', *Biomass and Bioenergy*, 153, p. 106215.
2. Aiazzi, B. *et al.* (2009) 'A comparison between global and context-adaptive pansharpening of multispectral images', *IEEE Geoscience and Remote Sensing Letters*, 6(2), pp. 302–306.
3. Curran, P. J. (1981) 'Multispectral remote sensing for estimating biomass and productivity', *Plants and the daylight spectrum*.
4. Gnanamoorthy, P. *et al.* (2019) 'Diurnal and seasonal patterns of soil CO₂ efflux from the Pichavaram mangroves, India', *Environmental monitoring and assessment*, 191(4), pp. 1–12.
5. Kathiresan, K. (2000) 'A review of studies on Pichavaram mangrove, southeast India', *Hydrobiologia*, 430(1), pp. 185–205.
6. Komiyama, A. *et al.* (2000) 'Top/root biomass ratio of a secondary mangrove (*Ceriops tagal* (Perr.) CB Rob.) forest', *Forest ecology and management*, 139(1–3), pp. 127–134.
7. Komiyama, A., Pongpan, S. and Kato, S. (2005) 'Common allometric equations for estimating the tree weight of mangroves', *Journal of tropical ecology*, 21(4), pp. 471–477.
8. Kurihara, H. and Shirayama, Y. (2004) 'Effects of increased atmospheric CO₂ on sea urchin early development', *Marine Ecology Progress Series*, 274, pp. 161–169.
9. Lehmann, J. (2007) 'A handful of carbon', *Nature*, 447(7141), pp. 143–144.
10. Li, Z. and Cheng, C. (2019) 'A CNN-based pan-sharpening method for integrating panchromatic and multispectral images using landsat 8', *Remote Sensing*, 11(22), p. 2606.
11. Myeong, S., Nowak, D. J. and Duggin, M. J. (2006) 'A temporal analysis of urban forest carbon storage using remote sensing', *Remote Sensing of Environment*, 101(2), pp. 277–282.
12. Pardo-Pascual, J. E. *et al.* (2012) 'Automatic extraction of shorelines from Landsat TM and ETM+ multi-temporal images with subpixel precision', *Remote Sensing of Environment*, 123, pp. 1–11.
13. Patil, V. *et al.* (2015) 'Estimation of Mangrove Carbon Stocks by Applying Remote Sensing and GIS Techniques', *Wetlands*. doi: 10.1007/s13157-015-0660-4.
14. Qi, J. *et al.* (1994) 'A modified soil adjusted vegetation index', *Remote Sensing of Environment*. doi: 10.1016/0034-4257(94)90134-1.
15. Ramanathan, A. L. *et al.* (1999) 'Environmental geochemistry of the Pichavaram mangrove ecosystem (tropical), southeast coast of India', *Environmental geology*, 37(3), pp. 223–233.
16. Sahu, S. C. *et al.* (2015) 'Mangrove area assessment in India: implications of loss of mangroves', *Journal of Earth Science & Climatic Change*, 6(5), p. 1.
17. Subramanian, P., Jeyaseelan, M. J. P. and Krishnamurthy, K. (1984) 'The nature of biodegradation of vegetation in mangrove ecosystem', *Chemistry in Ecology*, 2(1), pp. 47–68.
18. Yuen, J. Q. *et al.* (2013) 'Uncertainty in below-ground carbon biomass for major land covers in Southeast Asia', *Forest Ecology and Management*, 310, pp. 915–926.